A coupled Thermo-Hydro-Mechanical modeling of aperture closing and opening during heat extraction from fractured geothermal reservoir

Sachchida Nand Pandey and Abhijit Chaudhuri
Indian Institute of Technology Madras, Chennai-36, Tamil Nadu, India

Introduction

Reservoir deformation due to coupled thermal and hydraulic processes is important for various geological applications such as geothermal heat extraction, CO_2 sequestrations and nuclear waste disposal. The contraction of rock matrix and pore pressure increases during cold water injection into the reservoir, cause significant variation of reservoir porosity and permeability. In past, these evolutions were modeled considering either Thermo-Hydro-Mechanical effects [Kelkar 2014] or combined Thermo-Hydro-Mechanical-Chemical effects [Taron and Elsworth 2009]. When a large fracture/fault is the main flow conduits, the modeling of fracture opening and closing (i.e. aperture increase and decrease) is very important to predict long-term evolution of geothermal reservoir. Some past modeling studies quantified the coupled THM effects on the single fracture [Kohl et al. 1995; Rawal and Ghassemi 2014; Guo et al., 2015] and fracture networks [Koh et al. 2011; Fu et al, 2015]. Their result showed that cooling and overpressure resulted in reduction of effective normal stresses and increase in fracture aperture. All these studies indicated that couplings among the different physical processes occurred simultaneously, but at different time scales. Some processes such as thermo-elastic effects are present for the entire production period whereas poro-elastic effects are important in the early stage.

We performed coupled thermo-hydro-mechanical (THM) simulations to investigate the evolution of aperture of a single fracture connecting an injection and a production wells. We used FEHM code (Finite Element for Heat and Mass Transfer) for this purpose. The mass and energy balance equations in FEHM is solved using control volume method and force balance equations with finite element method. It was originally developed for modeling of heat & mass transfer and deformation of porous medium. But to make FEHM as capable of modeling of these processes for a facture, we considered fracture as an equivalent thin porous layer. The depth-integrated mass, momentum and energy transport in the porous layer were equated with those of the fracture [Chaudhuri et al., 2013]. This approach was successfully used for Thermo-Hydro-Chemical modeling of aperture alteration in geothermal setups [Pandey et al. 2014; 2015]. For the mechanical deformation of fracture, we implemented nonlinear fracture joint model in FEHM. For modeling of aperture alteration of fracture or rock joint, we considered Bandis model of stress dependent fracture stiffness. Form that we derived a nonlinear stress-strain relation for the equivalent porous layer to determine the permeability alteration.

Mathematical Model

The governing equation for poro-thermo-elastic deformation of rock matrix can be presented as Navier's equations with a hydraulic coupling term and a diffusion equation for the pore pressure [Rice and Cleary, 1976]:

$$\frac{E}{2(1+\nu)}\nabla^2\mathbf{u}+\frac{E}{2(1+\nu)(1-2\nu)}\nabla(\nabla.\mathbf{u})=-\rho_r\mathbf{g}-\beta\nabla P-\frac{\alpha E}{1-2\nu}\nabla(T-T_0) \text{ and } \frac{\partial P}{\partial t}=\frac{Mk}{\mu}\nabla^2P+\beta M\frac{\partial(\nabla\cdot\mathbf{u})}{\partial t} \quad (1)$$

where $\mathbf{u}$ and P are displacement vector of the rock and pore pressure respectively. Biot's coefficient, volumetric thermal expansion coefficient, Young's modulus and Poisson ratio are denoted by β, α, E and ν respectively. In pore pressure equation k, μ and M are permeability, viscosity and Biot modulus respectively. For flow and heat transfer through the fracture aperture-integrated equations [Pandey et al. 2014] were used. 3-D Darcy equation and convection-diffusion equation were used for porous rock matrix.

Bandis (1983) developed a hyperbolic model for fracture closure i.e. a relation between aperture deformation and effective normal stresses ($\sigma_n'=\sigma_n-P$) at the fracture plane.

$$\Delta b=b_{\max}-\frac{A\sigma_n'}{1+B\sigma_n'} \quad (2)$$

where A and B are mechanical properties of joint. $1/A$ is the initial normal stiffness and $b_{\max}$ is the maximum fracture closure at zero normal stress. The normal stiffness (K_n) of fracture joint is $K_n=(1+B\sigma_n')^2/A$. To model the fracture or rock joint as a deformable and thin porous layer, we derived the following expressions of the Young's modulus and strain (ε) of the equivalent porous medium as a function of effective normal stress,

$$E=\frac{d\sigma}{d\varepsilon}=\frac{b_{\max}(1+B\sigma_n')^2}{A} \text{ and } \varepsilon=\frac{\Delta b}{b_{\max}}=\frac{A\sigma_n'}{b_{\max}(1+B\sigma_n')} \quad (3)$$

At each time step, Young's modulus and aperture were calculated from the nodal value of σ_n'. The porosity and local permeability of equivalent porous layer were updated. These updated value of hydraulic and mechanical properties were used for simulation of flow, heat transport and deformation at next time step.

Results and discussions

To investigate the effect of cooling and fluid over pressure variations, we performed the several coupled Thermo-Hydro-Mechanical simulations of cold water injection into a geothermal reservoir (Fig. 1) for a period of 30 years. We considered the injection conditions as $T_{inj} = 50$ and $\dot{m} = 10$ kg/s while the joint stiffness and thermal expansion coefficients of the rock matrix were varied. The values of these parameters are listed in Table 1. Prior to discuss the effect of these parameters, we have presented the time evolution of temperature, effective stress, aperture and pressure fields along fracture plane in Figs. (2-5) respectively for $K_{ini} = 12$ GPa/m and $\alpha_T = 1\times10^{-4}$ 1/ ^{o}C.

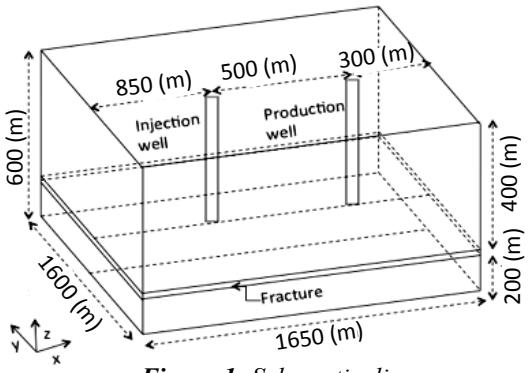

***Figure 1**: Schematic diagram*

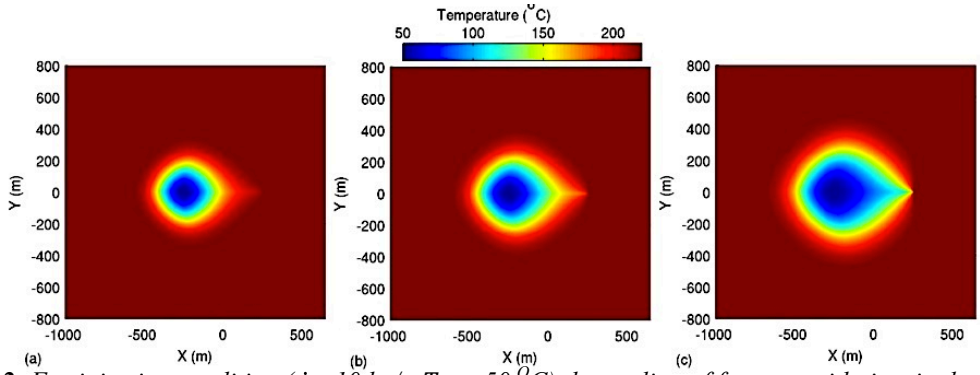

***Figure 2:** For injection condition ($\dot{m}$=10 kg/s, T_{inj}=50 ^{O}C) the cooling of fracture with time is shown by plotting temperature fields at different time instances: (a) 5 years, (b) 10 years, and (c) 30 years. These results are for reservoir rock/fracture properties as $K_{ini} = 12$ GPa/m and $\alpha_T = 1\times10^{-4}$ 1/ ^{o}C.*

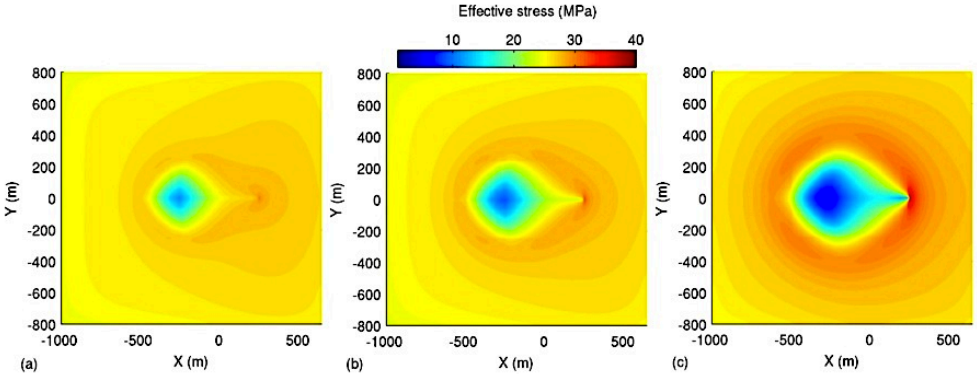

***Figure 3**: For injection condition ($\dot{m}$=10 kg/sand T_{inj} = 50 ^{O}C) the change of effective stress distribution at the fracture surface with time due to cooling is shown by plotting the effective stress field at different time instances, (a) 5 years, (b) 10 years, and (c) 30 years.*

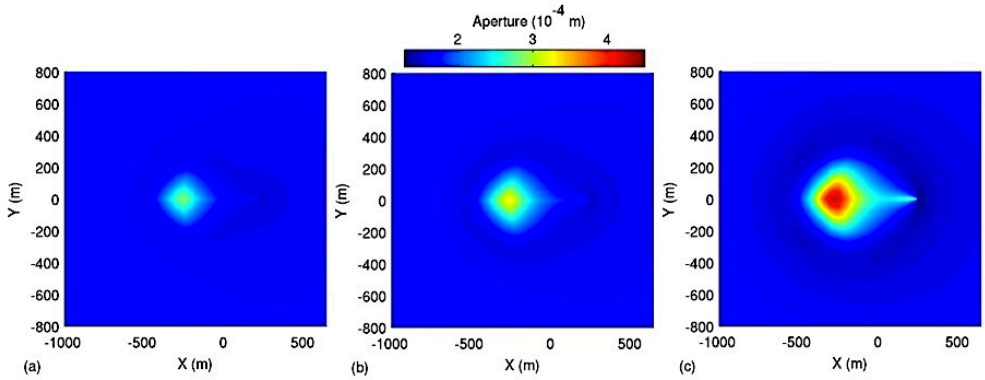

***Figure 4**: For injection condition ($\dot{m}$=10 kg/sand T_{inj} = 50 ^{O}C) the alteration of aperture of the fracture with time is shown by plotting the aperture field at different time instances, (a) 5 years, (b) 10 years, and (c) 30 years.*

In the beginning of the operation, the temperature drop occurs in the vicinity of the injection well. The expansion of cold zone with time is very clear from Figs. (2a -2c). The temperature drawdown in the production well is plotted in Fig. 6a. This figure shows that the thermal break through occurred after 2.5 years. Afterward T_{pro} temperature was dropping very steadily with time almost at a constant rate. However the area of cooling

within the fracture does not increase much (see Fig. 2) rather remains confined within a zone of approximately of 400 m radius. This implies that the flow was confined in a smaller area of the fracture. This is due to facture opening and closing as seen Fig. (4). Fracture opening and closing were due to the spatio-temporal variation of effective stress as shown in Fig. (3a-3c). Alteration aperture caused the spatial and temporal variation of local transmissivity field because it is proportional to b^3. That resulted in the variation of fluid pressure gradient with time. This can be realized from the temporal variations of pressure contour in Fig. (5). Aperture growth at the middle of the fracture enhanced effective transmissivity and reduced the flow impedance as seen in Fig. (6c). The energy output in Fig. (6b) followed the similar decline as production temperature. The faster drop of production temperature and rate of energy output in the case THM modeing were caused by flow channeling.

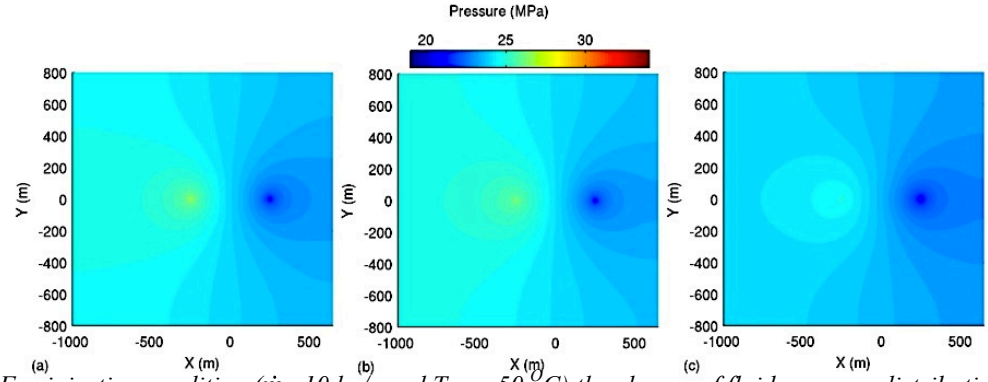

Figure 5: For injection condition ($\dot{m}$=10 kg/s and T_{inj} = 50 ^{O}C) the change of fluid pressure distribution inside fracture with time is shown by plotting the pressure field at different time instances, (a) 5 years, (b)10 years, and (c) 30 years.

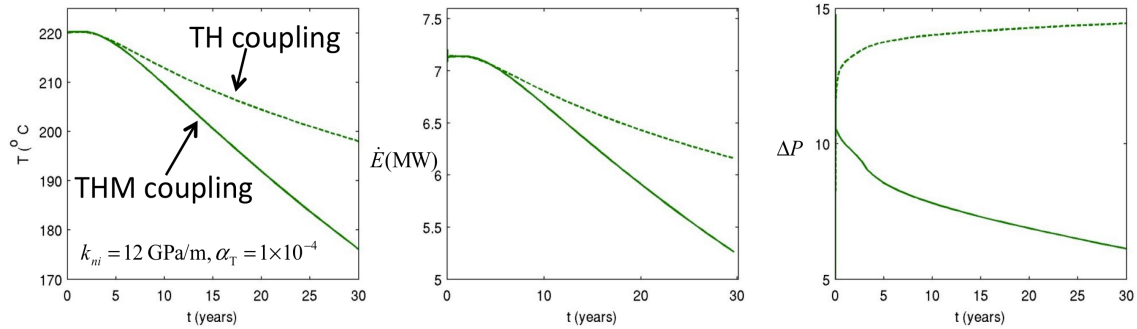

***Figure 6:**. The effects of aperture alteration by thermal contraction and fluid overpressure are shown by comparing the temporal variations of TH and THM coupling results: (a) temperature at the production well, (b) energy flux, and (c) pressure difference between injection and production wells.*

Table 1: Properties of rock matrix, joint and fluid

Parameter	Value
Initial fracture aperture for fluid flow (mm)	0.147
Rock permeability (m^2)	1×10^{-18}
Rock density (kg/m^3)	2500
Fluid heat capacity (J/kg/K))	4180
Rock heat capacity (J/kg/K)	1000
Rock thermal conductivity (W/m/K)	2.5
Fluid thermal conductivity (W/m/K)	0.6
Young's modulus of rock (GPa)	15
Poisson's ratio of rock	0.3
Biot's coefficient of rock	0.7
Volumeric coefficient thermal expansion (1/^{O}C)	3×10^{-5} and 1×10^{-4}
Joint stiffness (GPa/m)	12 and 100
Mass flow rate (kg/s)	10
Injection temperature (^{O}C)	50

Effect of joint stiffness and thermal expansion coefficient of rock:

As expected, the increase of joint stiffness leads to higher resistance to opening and closure of the fracture. The effective stress and aperture distribution along the fracture after 30 years are shown in Figs. (7a) and (7b) respectively for $K_{ini} = 100$ GPa/m. For both value of joint stiffness the initial aperture were same. Figure (7a) shows that the maximum and minimum values of effective stress developed due to cooling and over fluid pressure for higher stiffness are very close to those seen in Fig. (3c) for lower stiffness. But Fig. (7b) shows that

the aperture increase near the injection well for $K_{ini} = 100$ GPa/m is approximately 1/4th of that of $K_{ini} = 12$ GPa/m.

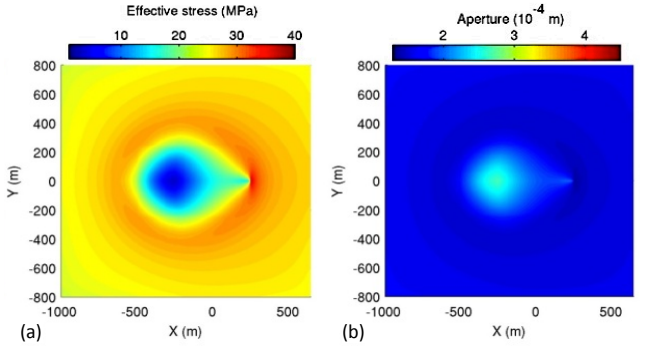

Figure 7: *To show the effect of joint stiffness on the aperture alteration, (a) effective stress and (b) aperture after 30 years are plotted for joint stiffness ($K_{ini} = 100$ GPa/m) and thermal expansion coefficient ($\alpha_T = 1\times10^{-4}$ 1/^{O}C).*

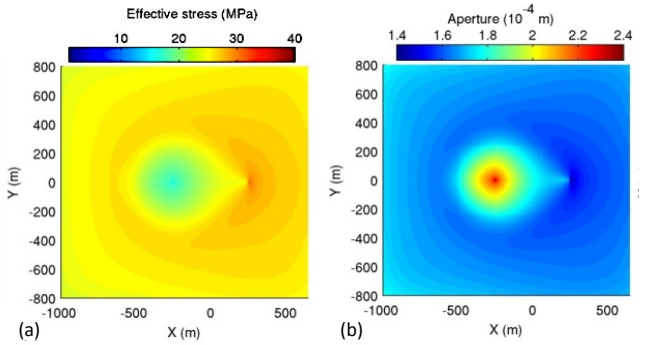

Figure 8: *To show the effect of joint stiffness on the aperture alteration, (a) effective stress and (b) aperture after 30 years are plotted for joint stiffness ($K_{ini} = 12$ GPa/m) and thermal expansion coefficient ($\alpha_T = 3\times10^{-5}$ 1/^{O}C).*

The contraction of rock matrix is directly proportional to the linear thermal expansion coefficient (α_T). Hence thermal expansion coefficient strongly influences the aperture alteration during cold water injection into the reservoir. Figure (8a) shows that range of effective stress were significantly smaller for smaller value of α_T. Figure (8b) shows that the maximum increase of aperture near the injection well was approximately three times lower for $\alpha_T = 3\times10^{-5}$ 1/^{O}C than for $\alpha_T = 1\times10^{-4}$ 1/^{O}C (see Fig. 4c).

Summary and conclusions

The effects of Thermo-Hydro-Mechanical deformation of rock matrix and joint on the heat extraction process and injection pressure are discussed. In the present approach rock joint/fracture is modeled as an equivalent porous medium. The porosity, permeability and stiffness are updated according to the effective stress as determined by solving coupled Thermo-Hydro-Mechanical equations. Our simulation showed fracture opening near injection well and closer in the outer region, which is know as thermal caging in geothermal literature. Aperture growth causes reduction of injection pressure but faster temperature drawdown in the production well. The aperture growth is very sensitive to the joint stiffness and thermal expansion coefficient.

References

1. Chaudhuri A., Rajaram H. and Viswanathan H., 2013. Early-stage hypogene karsti- fication in a mountain hydrologic system: a coupled thermo-hydro-chemical model incorporating buoyant convection. Water Resources Research 49, http://dx.doi.org/10.1002/wrcr.20427.
2. Fu P., Hao Y., Walsh S. D. C. and Carrigan C. R., 2015. Thermal Drawdown-Induced Flow Channeling in Fractured Geothermal Reservoirs. Rock Mech Rock Eng., DOI 10.1007/s00603-015-0776-0.
3. Guo B., Fu P., Hao Y., Carrigan C.R., 2015, Thermal Drawdown-induced Flow Channeling in A Single Heterogeneous Fracture in Geothermal Reservoir, PROCEEDINGS, Fourtieth Workshop on Geothermal Reservoir Engineering Stanford University, Stanford, California, January 26-28, 2015
4. Kelkar S., Lewis K, Karra S., Zyvoloski G, Rapaka S., Viswanathan H., Mishra P.K., Chu S., Coblentz D. and Pawar R., 2014. A simulator for modeling coupled thermo-hydro-mechanical processes in subsurface geological media. International Journal of Rock Mechanics & Mining Sciences 70, 569–580.
5. Koh J, Roshan H. and Rahman SS., 2011. A numerical study on the long term thermo-poroelastic effects of cold water injection into naturally fractured geothermal reservoirs. Comput Geotech 38, 669–682.
6. Kohl T., Evansi K, Hopkirk R, and Rybach L., 1995. Coupled hydraulic thermal and mechanical considerations for the simulation of hot dry rock reservoirs. Geothermics 24, 345–359.
7. Pandey S.N., Chaudhuri A., Kelkar S., Sandeep V.R. and Rajaram H. 2014,. Investigation of permeability alteration of fractured limestone reservoir due to geothermal heat extraction using three-dimensional thermo-hydro-chemical (THC) model. Geothermics 51, 46– 62.
8. Pandey S.N., Chaudhuri A., Rajaram H. and Kelkar S., 2015. Fracture transmissivity evolution due to silica dissolution/precipitation during geothermal heat extraction. Geothermics 57, 111-126.
9. Rawal C. and Ghassemi A, 2014. A reactive thermo poroelastic analysis of water injection into an enhanced geothermal reservoir. Geothermics 50, 10–23.
10. Taron J. and Elsworth D., 2009. Thermal–hydrologic–mechanical–chemical processes in the evolution of engineered geothermal reservoirs, International Journal of Rock Mechanics and Mining Sciences 46, 855-864.